Quantum Dots Attached to Ferromagnetic Leads: Exchange Field, Spin Precession, and Kondo Effect

Jürgen König[1], Jan Martinek[2,3,4], Józef Barnaś[4,5], and Gerd Schön[2]

[1] Institut für Theoretische Physik III, Ruhr-Universität Bochum, 44780 Bochum, Germany
[2] Institut für Theoretische Festkörperphysik, Universität Karlsruhe, 76128 Karlsruhe, Germany
[3] Institute for Materials Research, Tohoku University, Sendai 980-8577, Japan
[4] Institute of Molecular Physics, Polish Academy of Sciences, 60-179 Poznań, Poland
[5] Department of Physics, Adam Mickiewicz University, 61-614 Poznań, Poland

Abstract. Spintronics devices rely on spin-dependent transport behavior evoked by the presence of spin-polarized electrons. Transport through nanostructures, on the other hand, is dominated by strong Coulomb interaction. We study a model system in the intersection of both fields, a quantum dot attached to ferromagnetic leads. The combination of spin-polarization in the leads and strong Coulomb interaction in the quantum dot gives rise to an exchange field acting on electron spins in the dot. Depending on the parameter regime, this exchange field is visible in the transport either via a precession of an accumulated dot spin or via an induced level splitting. We review the situation for various transport regimes, and discuss two of them in more detail.

1 Introduction

The study of spin-dependent tunneling through quantum dots resides in the intersection of two active and attractive fields of physics, namely spintronics [1–3] and transport through nanostructures [4–6]. Both the investigation of spin-dependent electron transport on the one hand and the study of strong Coulomb interaction effects in transport through nanostructures on the other hand define by now well-established research areas. The combination of both concepts within one system is, however, a very new field which is still in its early stages. Its attractiveness originates from the rich physics expected from the combination of two different paradigms. A suitable model system for a basic study of the interplay of spin-dependent transport due to spin polarization in ferromagnetic electrodes and Coulomb charging effects in nanostructures is provided by a quantum dot attached to ferromagnetic leads.

1.1 Some Concepts of Spintronics

The field of spin- or magnetoelectronics [1–3] has attracted much interest, for both its beautiful fundamental physics and its potential applications. A famous example, which has already proven technological relevance, is the spin valve

based on either the giant magnetoresistance effect (GMR) in magnetic multilayers or the tunnel magnetoresistance (TMR) in magnetic tunnel junctions. In both cases, the transport properties depend on the relative magnetization orientation of the involved magnetic layers or leads, an information conveyed by the spin polarization of the transported electrons. In the case of a single magnetic tunnel junction, the tunneling current is maximal for parallel alignment of the leads' magnetization orientations, while it is minimal for antiparallel alignment. This can be easily understood within a non-interacting-electron picture, as proposed by Jullière [7]: the tunnel current of electrons with given spin direction is proportional to the product of the corresponding spin-dependent densities of states in the source and drain electrode, which leads to a reduction of transport in the case of antiparallel alignment.

This concept has been extended [8] to describe also noncollinear arrangements, as depicted in Fig. 1(a), where the magnetization directions of the leads enclose an arbitrary angle ϕ. In this situation, the ϕ-dependent part of the tunneling current is proportional to the overlap of the spinor part of the majority-spin wave functions in the source and drain electrode, i.e. proportional to $\cos\phi$, as it has been experimentally confirmed recently [9].

In heterostructures that consist of a nonmagnetic metal sandwiched by ferromagnetic electrodes, the concept of spin accumulation becomes important. Once the spin diffusion length is larger than the size of the nonmagnetic region, the information about the relative orientation of the leads' magnetization is mediated through the middle part. In the antiparallel configuration an applied bias voltage leads to a pile up of spin in the nonmagnetic metal, since electrons with one type of spin (say spin up) are preferentially injected from the source electrode, while electrons with the other type of spin (spin down) are pulled out from the drain electrode. This piling up of spin splits the chemical potentials for spin-up and spin-down electrons in the normal metal such that electrical transport through the whole device is reduced.

As spin is a vector quantity, transport through a ferromagnetic-nonmagnetic-ferromagnetic heterostructure can be tuned by manipulating the direction of the spins in the middle part. The prototype for such a concept is the spin field-effect transistor proposed by Datta and Das [10]. Spin-polarized electrons are injected from a ferromagnetic metal into a ballistic conducting channel provided by a two-dimensional electron gas in a semiconductor heterostructure. Due to the Rashba effect, the electrons in the semiconductor experience a spin-orbit coupling, whose strength can be tuned by a gate voltage. This spin-orbit coupling leads to a rotation of the spins in the conducting channel as they move along towards the drain electrode. The total transmission through the device, then, depends on the relative orientation of the rotated spins and the magnetization direction of the drain electrode.

1.2 Transport Through Nanostructures

Tunneling transport through nanostructures, such as semiconductor quantum dots (Fig. 1(b)) or small metallic islands, is strongly affected by Coulomb in-

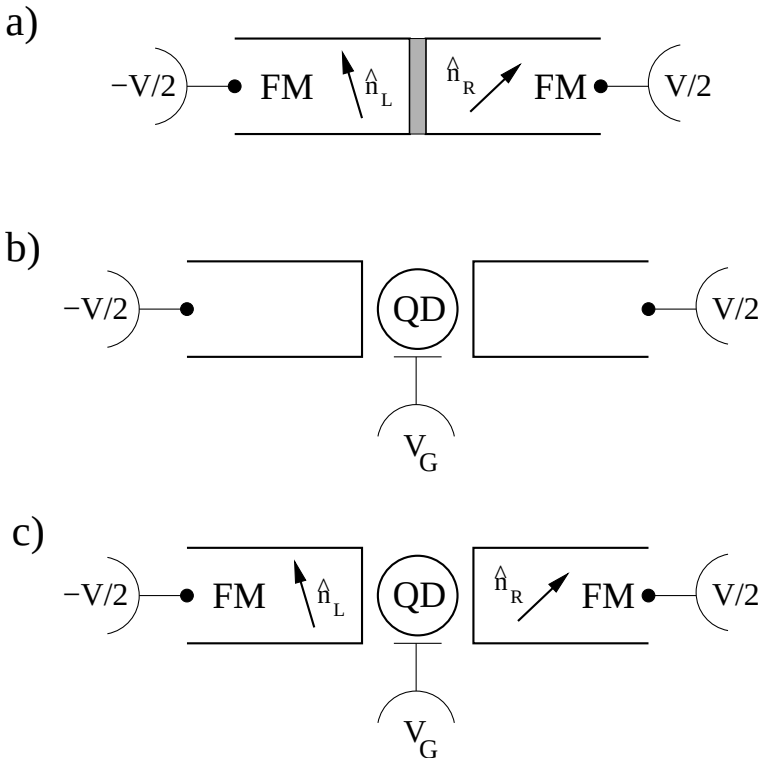

Fig. 1. a) Spin valve: a single tunnel junction between two ferromagnets (FM) with magnetization orientations $\hat{\mathbf{n}}_{\mathrm{L}}$ and $\hat{\mathbf{n}}_{\mathrm{R}}$, respectively. b) Quantum dot. c) Quantum-dot spin valve: a quantum dot is connected to two ferromagnetic leads (FM)

teraction, and a non-interacting electron picture is no longer applicable [4–6]. Coulomb-blockade phenomena arise at low temperature, such that the corresponding energy scale is smaller than the charging energy, the energy scale for adding or removing one electron from the dot or island. Small quantum dots with a size of the order of the Fermi wavelength have a discrete level spectrum. If the level spacing is large enough, transport through single levels is possible. This situation defines a simplest but very generic model, the Anderson-impurity model, for studying Coulomb interaction in nanostructures.

When the level is occupied with one electron since double occupancy is prohibited by charging energy, the dot possesses a local spin. At low temperature and large dot-lead tunnel-coupling strength, a ground state with complex many-body correlations forms, which manifests itself in the so-called Kondo effect [11]. The local spin is screened by the spins of the conduction electrons in the leads, and accompanied with this, electrical transport through the quantum dot is strongly enhanced.

1.3 Quantum-Dot Spin Valves

The scheme of a quantum-dot spin valve, a quantum dot attached to ferromagnetic leads, is illustrated in Fig. 1(c). Successful fabrication of either quantum-dot systems or magnetic heterostructures has been achieved by a large number of experimental groups. To attach ferromagnetic electrodes to quantum dots, though, is quite a challenging task, and only very recently first results have been reported.

Let us start with metallic single-electron devices. Both spin-dependent tunneling and Coulomb blockade has been found in magnetic tunnel junction with embedded Co clusters [12]. All-ferromagnetic metallic single-electron transistors have been manufactured, using either single-island [13,14], or multi-island structures [15,16]. Magnetoresistance of single-electron transistors with a normal metallic island in a cobalt-aluminum-cobalt structure has been measured [17]. In all these examples, the level spectrum on the island is continuous, and many levels are involved in transport.

Our focus, however, is on single-level quantum dots. The difficulty lies in the incompatibility of the usual materials showing ferromagnetism (metals) and those usually forming quantum dots (semiconductors). There are different strategies to overcome this problem. One possibility is the use of ferromagnetic semiconductors (Ga,Mn)As as lead electrodes coupled to, e.g., self-assembled InAs quantum dots [18]. A very promising approach is to contact an ultrasmall aluminum nanoparticle, which serves as a quantum dot, to ferromagnetic metallic electrodes. In this way, quantum dots with one magnetic (nickel or cobalt) and one nonmagnetic (aluminum) electrodes have been fabricated [19]. Another important system is a magnetic impurity inside the tunneling barrier of ferromagnetic tunnel junction [20]. An alternative route is to use carbon nanotubes as quantum dots and to place them on metallic contacts. Coulomb-blockade phenomena and even the Kondo effect has been observed in such systems [21,22]. Spin-dependent transport through carbon nanotubes attached to ferromagnetic electrodes has been investigated in [23,24]. A more challenging scheme is a ferromagnetic single-molecule transistor [25], where a single molecule is attached to ferromagnetic electrodes. To some extent, there is also a relation between the quantum-dot spin valve and a single magnetic-atom spin on a scanning tunneling microscope tip. For the latter, precession of the single spin in an external magnetic field has been detected in the power spectrum of the tunneling current [26].

This progress on the experimental side has stimulated a number of theoretical activities [27–40] on spin-dependent transport through either metallic single-electron transistors or quantum dots.

The motivation for studying quantum-dot spin valves can be formulated from two different perspectives, depending on from which side one starts to approach the problem. Coming from the spintronics side, one may ask how the concepts introduced there, such as spin accumulation and spin manipulation, manifest themselves in quantum dots, and how the presence of strong Coulomb interaction gives rise to qualitatively new behavior as compared to non-interacting electron

systems. On the other hand, when starting from Coulomb-interaction effects in quantum dots, one may ask how the spin-polarization of the leads changes the picture. As mentioned above, the screening of a local spin on the quantum dot by the lead-electron spins is crucial for the Kondo effect to develop. This screening behavior is affected by spin asymmetry introduced due to a finite spin polarization of the lead. In this case, it is a priori not clear whether a Kondo-correlated state can still form or not.

To comprise all this in a single question, we ask whether the combination of strong Coulomb interaction and finite spin-polarization gives rise to qualitatively new phenomena that are absent for either non-interacting or unpolarized electrons. The answer is: yes, it does. We predict that single electrons on the quantum dot experience an exchange field, which effectively acts like a local magnetic field. The main goal of this paper is to illustrate the origin of this exchange field, its properties, and its implications on transport. Of course, the latter depends on the considered transport regime, and the observable consequences can be quite different. In the present paper, we concentrate on two particular regimes, the case of weak dot-lead coupling but noncollinear magnetization directions and the case of very strong coupling but collinear configuration. Other limits will only be commented on shortly, as for these cases work is still in progress and will be presented elsewhere.

2 The Model

We consider a small quantum dot with one energy level ϵ participating in transport. The dot is coupled to ferromagnetic leads, see Fig. 1(c). The left and right lead are magnetized along $\hat{\mathbf{n}}_{\mathrm{L}}$ and $\hat{\mathbf{n}}_{\mathrm{R}}$, respectively. The total Hamiltonian is

$$H = H_{\mathrm{dot}} + H_{\mathrm{L}} + H_{\mathrm{R}} + H_{\mathrm{T,L}} + H_{\mathrm{T,R}} \,. \tag{1}$$

The first part, $H_{\mathrm{dot}} = \epsilon \sum_\sigma c_\sigma^\dagger c_\sigma + U n_\uparrow n_\downarrow$, describes the dot energy level plus the charging energy U for double occupation. In the presence of an external magnetic field, the energy level experiences a Zeeman splitting, i.e., becomes spin-dependent. The leads are modeled by $H_r = \sum_{k\sigma} \epsilon_{k\sigma} a_{rk\sigma}^\dagger a_{rk\sigma}$ with $r = \mathrm{L}, \mathrm{R}$. In the spirit of a Stoner model of ferromagnetism [41], there is a strong spin asymmetry in the density of states $\rho_{r\sigma}(\omega)$ for majority ($\sigma = +$) and minority ($\sigma = -$) spins. Throughout all of our calculations presented here, we approximate the density of states to be energy independent, $\rho_{r\sigma}(\omega) = \rho_{r\sigma}$. Real ferromagnets will have a structured density of states [42]. This fact, however, will only modify details of the results and not the main physical picture. The ratio $p = (\rho_{r+} - \rho_{r-})/(\rho_{r+} + \rho_{r-})$ characterizes the degree of spin polarization in the leads. For simplicity, we assume here $\rho_{\mathrm{L}+} = \rho_{\mathrm{R}+} \equiv \rho_+$ and $\rho_{\mathrm{L}-} = \rho_{\mathrm{R}-} \equiv \rho_-$. Nonmagnetic leads are described by $p = 0$, and $p = 1$ represents half metallic leads, which accommodate majority spins only. We emphasize that the magnetization directions of leads can differ from each other, enclosing an angle ϕ.

Tunneling between leads and dot is described by the standard tunneling Hamiltonian. For the left tunnel barrier we get

$$H_{\mathrm{T,L}} = t \sum_{k\sigma=\pm} \left(a^\dagger_{\mathrm{L}k\sigma} c_\sigma + h.c. \right) , \tag{2}$$

where $c_\pm$ are the Fermi operators for an electron on the quantum dot with spin along $\pm\hat{\boldsymbol{n}}_r$. For the right barrier, an analogous expression holds. As $\hat{\boldsymbol{n}}_{\mathrm{L}}$ may differ from $\hat{\boldsymbol{n}}_{\mathrm{R}}$, an ambiguity arises in the definition of $c_\pm$. This is no problem for collinear, i.e., parallel or antiparallel, configuration of the leads. In this case, $\hat{\boldsymbol{n}}_{\mathrm{L}} = \pm\hat{\boldsymbol{n}}_{\mathrm{R}}$ provides a natural quantization axis for the dot spin.

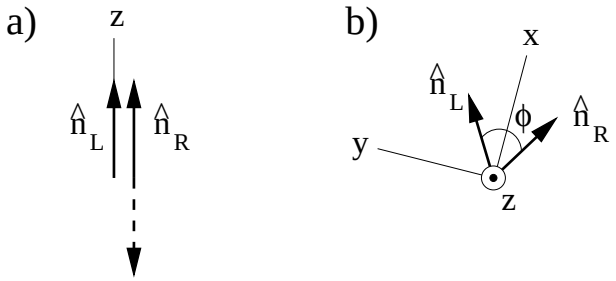

Fig. 2. Choice of the used coordinate system: a) For collinear configuration of the leads' magnetization, i.e., parallel (solid arrow for $\hat{\boldsymbol{n}}_{\mathrm{R}}$) or antiparallel (dashed arrow), the z-axis is along $\hat{\boldsymbol{n}}_{\mathrm{L}}$. In this case, we use the tunneling Hamiltonian in the form of (2). b) For noncollinear arrangements, the z-axis is perpendicular to both $\hat{\boldsymbol{n}}_{\mathrm{L}}$ and $\hat{\boldsymbol{n}}_{\mathrm{R}}$. Here, the tunneling Hamiltonian in the form of (3) is used. The quantum-dot spin is always quantized along the z-axis

For noncollinear leads, however, the form (2) of the tunnel Hamiltonian is no longer useful. To describe the scenario properly, we find it convenient to quantize the dot spin neither along $\hat{\boldsymbol{n}}_{\mathrm{L}}$ nor $\hat{\boldsymbol{n}}_{\mathrm{R}}$, but along the axis perpendicular to both $\hat{\boldsymbol{n}}_{\mathrm{L}}$ and $\hat{\boldsymbol{n}}_{\mathrm{R}}$. To be explicit, we choose the coordinate system defined by $\hat{\boldsymbol{e}}_x = (\hat{\boldsymbol{n}}_{\mathrm{L}} + \hat{\boldsymbol{n}}_{\mathrm{R}})/|\hat{\boldsymbol{n}}_{\mathrm{L}} + \hat{\boldsymbol{n}}_{\mathrm{R}}|$, $\hat{\boldsymbol{e}}_y = (\hat{\boldsymbol{n}}_{\mathrm{L}} - \hat{\boldsymbol{n}}_{\mathrm{R}})/|\hat{\boldsymbol{n}}_{\mathrm{L}} - \hat{\boldsymbol{n}}_{\mathrm{R}}|$, and $\hat{\boldsymbol{e}}_z = (\hat{\boldsymbol{n}}_{\mathrm{R}} \times \hat{\boldsymbol{n}}_{\mathrm{L}})/|\hat{\boldsymbol{n}}_{\mathrm{R}} \times \hat{\boldsymbol{n}}_{\mathrm{L}}|$, and quantize the dot spin along the z-direction, see Fig. 2. The tunnel Hamiltonian, then, becomes

$$H_{\mathrm{T,L}} = \frac{t}{\sqrt{2}} \sum_k (a^\dagger_{\mathrm{L}k+}, a^\dagger_{\mathrm{L}k-}) \begin{pmatrix} e^{i\phi/4} & e^{-i\phi/4} \\ e^{i\phi/4} & -e^{-i\phi/4} \end{pmatrix} \begin{pmatrix} c_\uparrow \\ c_\downarrow \end{pmatrix} + h.c. , \tag{3}$$

and $H_{\mathrm{T,R}}$ is the same but with $\mathrm{L} \to \mathrm{R}$ and $\phi \to -\phi$. The special choice of the coordinate system implies that both up and down spins of the dot are equally-strongly coupled to the majority and minority spins of the leads. There, are, however, phase factors $e^{\pm i\phi/4}$ are involved, similar to multiply-connected quantum-dot systems dubbed Aharonov-Bohm interferometers [43]. The two spin directions $\uparrow$ and $\downarrow$ in the dot correspond to the quantum dots placed in the two arms of the Aharonov-Bohm interferometer, and the angle ϕ plays the role of the Aharonov-Bohm phase, which measures the total magnetic flux enclosed by the arms of the interferometer in units of the flux quantum. We note,

however, that our model translates to a very special kind of Aharonov-Bohm interferometer: the dot in each interferometer arm accommodates only a single level instead of a doubly-degenerate one, and Coulomb interaction occurs between the two dots, instead of within each of them.

The two different choices we use for the collinear and noncollinear configuration, in which we use either (2) or (3), respectively, are illustrated in Fig. 2. In both cases, the tunnel coupling leads to a finite width of the dot level. Its energy scale is given by $\Gamma = \sum_r \Gamma_r$ with $\Gamma_r = \pi|t|^2 \sum_{\sigma=\pm} \rho_\sigma$ [44].

3 Exchange Field

As pointed out in the introduction, the qualitative new physics introduced by the combination of spin-polarized leads and strong Coulomb interaction in the dot, is the existence of an exchange field acting on electron spins in the dot. This exchange field is intrinsically present in the model described by the Hamiltonian (1) together with the spin-dependent density of states. It is, therefore, automatically contained in any consistent treatment of the model for a given transport regime, as we will see in the subsequent sections. Nothing has to be added by hand. Nevertheless, we find it instructive to derive an explicit analytic expression by making use of the following heuristic procedure.

Each of the two leads will contribute to the exchange field separately. To keep the discussion transparent, we consider the effect of one lead only. The total exchange field is, then, just the sum over both leads. The first step is to derive an effective Hamiltonian for the subspace of the total Hilbert space in which the quantum dot is singly occupied. This is the regime of interest, as far as the exchange field in concerned, since both an empty and a doubly-occupied dot have zero total spin, and an exchange field would be noneffective. By taking into account virtual excitations to an empty or doubly-occupied dot within lowest-order perturbation theory in the tunnel coupling, in analogy to the Schrieffer-Wolff transformation [11] employed in the context of Kondo physics for magnetic impurities in nonmagnetic metals, we arrive at an effective spin model for the dot spin operators $S^{\pm}$ and S^z (quantized along the magnetization direction of the considered lead),

$$\begin{aligned} H_{\rm spin} = {} & S^+|t|^2 \sum_{kq} \left(\frac{1}{U+\epsilon-\epsilon_q} + \frac{1}{\epsilon_k-\epsilon} \right) a^\dagger_{rk\downarrow} a_{rq\uparrow} \\ & + S^-|t|^2 \sum_{kq} \left(\frac{1}{U+\epsilon-\epsilon_k} + \frac{1}{\epsilon_q-\epsilon} \right) a^\dagger_{rq\uparrow} a_{rk\downarrow} \\ & + S^z|t|^2 \left(\sum_{qq'} \frac{1}{U+\epsilon-\epsilon_{q'}} a^\dagger_{rq\uparrow} a_{rq'\uparrow} - \sum_{kk'} \frac{1}{U+\epsilon-\epsilon_{k'}} a^\dagger_{rk\downarrow} a_{rk'\downarrow} \right) \\ & - S^z|t|^2 \left(\sum_{qq'} \frac{1}{\epsilon_q-\epsilon} a_{rq'\uparrow} a^\dagger_{rq\uparrow} - \sum_{kk'} \frac{1}{\epsilon_k-\epsilon} a_{rk'\downarrow} a^\dagger_{rk\downarrow} \right) . \end{aligned} \tag{4}$$

Note, that the information about the different densities of states for up- and down-spins is included in the summation over q, q' (used for spin-up electrons) and k, k' (used for spin down), respectively. In addition, there is a term describing potential scattering, but this does not contribute to the exchange field we are aiming at.

In a second step we employ in (4) a mean-field approximation for the lead-electron states, making use of $\langle a^\dagger_{rk\sigma} a_{rk'\sigma'}\rangle = f_r(\epsilon_{k\sigma})\delta_{kk'}\delta_{\sigma\sigma'}$ and $\langle a_{rk\sigma} a^\dagger_{rk'\sigma'}\rangle = [1 - f_r(\epsilon_{k\sigma})]\delta_{kk'}\delta_{\sigma\sigma'}$, where $f_r(\omega)$ is the Fermi function of lead r. The terms proportional to $S^\pm$ drop out. The resulting effective Hamiltonian, then, reads $H_{\rm eff} = -S^z B_r$ with the exchange field (for simplicity we include the gyromagnetic factor in the definition)

$$B_r = \int' d\omega(\rho_+ - \rho_-)|t|^2 \left(\frac{1 - f_r(\omega)}{\omega - \epsilon} + \frac{f_r(\omega)}{\omega - \epsilon - U}\right) \tag{5}$$

$$= -\frac{p\Gamma_r}{\pi}\mathrm{Re}\left[\Psi\left(\frac{1}{2} + i\frac{\beta(\epsilon - \mu_r)}{2\pi}\right) - \Psi\left(\frac{1}{2} + i\frac{\beta(\epsilon + U - \mu_r)}{2\pi}\right)\right], \tag{6}$$

where $\Psi(x)$ denotes the digamma function, μ_r is the electrochemical potential of lead r, and the prime at the integral sign in (5) symbolizes Cauchy's principal value. For illustration, we plot the exchange field as a function of the level position in Fig. 3.

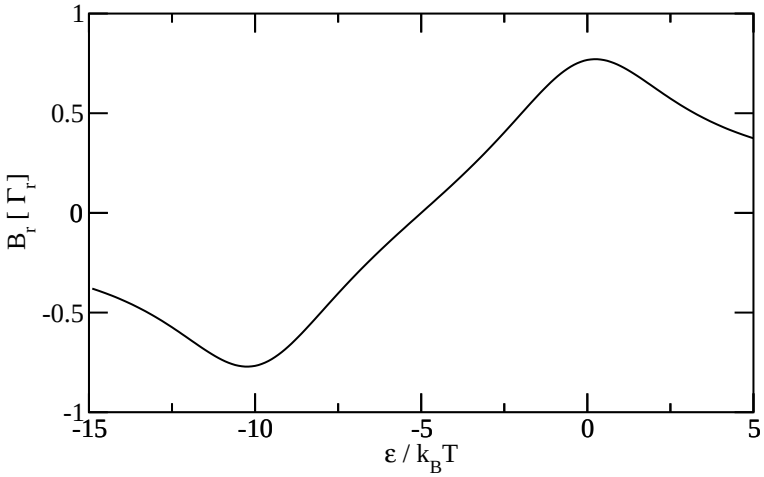

Fig. 3. The exchange field as a function of the level position ϵ for $U/k_{\rm B}T = 10$ and $p = 1$

From the explicit form (6) of the exchange field we derive the following properties:

(i) It vanishes in the case of a non-interacting quantum dot, $U = 0$.

(ii) The exchange field is proportional to the degree of spin-polarization p in the lead. This means that both strong Coulomb interaction and finite spin-polarization are required to generate the exchange field.
(iii) It depends on the tunnel coupling strength Γ. In the treatment lined out above, Γ enters linearly as a global prefactor.
(iv) The magnitude and even the sign of the exchange field depends on the level position ϵ. In particular, there is a value of ϵ at which the exchange field vanishes (in our model with flat density of states this happens at $\epsilon - \mu_r = U/2$, i.e., when the total system is particle-hole symmetric).

Furthermore, we notice from (5) that not only electronic states around the Fermi energy of the lead are involved. Instead, it is rather the full band that matters. This means, that a precise simulation of realistic materials requires a knowledge of the detailed density of states, to be inserted in the integral in (5). This will modify the details of the exchange field such as its precise dependence on the level position ϵ.

4 Transport Regimes

After introducing the notion of the exchange field, the question of how it affects the transport behavior arises immediately. The answer to this question depends on the transport regime under consideration. In particular, we will identify two mechanisms by which the exchange field enters. One scenario is the generation of a level splitting between up and down spins in the quantum dot, with the level splitting given by the exchange field (6). But this is not the only possibility. Even in situations, in which the generated level splitting is negligible, the exchange field can affect the dot state and, thus, the transport behavior by rotating an accumulated spin on the dot, which can pile up there in non-equilibrium due to an applied bias voltage. A complete picture of the various different transport regimes goes beyond the scope of the present paper. Instead, we will concentrate on two specific limits, namely weak dot-lead coupling but noncollinear magnetization in linear response, and strong coupling but collinear configuration of the leads. For some other regimes, that are currently under investigation, we will only give some short comments and refer the reader to forthcoming publications.

In the limit of weak dot-lead coupling, $\Gamma \ll k_{\mathrm{B}}T$, referred to as sequential-tunneling regime, transport is dominated by processes of first order in Γ (unless both ϵ and $\epsilon + U$ are shifted into the Coulomb-blockade region). First-order transport probes the state of the quantum dot to zeroth order (since the tunneling between dot and leads necessary for transport already trivially involves a factor Γ). Therefore, the level splitting generated by the exchange field cannot be probed by first-order transport. Nevertheless, the exchange field plays a role via the second of the above mentioned mechanisms. Once a finite spin is accumulated on the quantum dot, with a direction noncollinear to the exchange field, the latter will induce a precession of the accumulated spin. For this to happen, a noncollinear configuration of the leads' magnetic moments is required, as

otherwise accumulated spin, if any, and exchange field are pointing in the same direction.

In the Coulomb-blockade regime, sequential tunneling is exponentially suppressed, and transport is dominated by cotunneling, which are second-order processes. But also on resonance, second-order corrections become important for intermediate coupling strengths, $\Gamma \sim k_{\rm B}T$. Second-order transport is affected by the generated level splitting, and the exchange field plays a role even for a collinear arrangement of the leads' magnetization.

A very dramatic signature of the level splitting generated by the exchange field is predicted for the limit of low temperature and large coupling strength, $k_{\rm B}T \leq k_{\rm B}T_{\rm K} \ll \Gamma$, for which the Kondo effect can appear ($T_{\rm K}$ is the Kondo temperature). Since a finite level splitting, e.g., due to a Zeeman term induced by an external magnetic field, quickly destroys the Kondo effect, the exchange field has quite an important, at first glance destructive, consequence. As we will see below in more detail, however, by applying an appropriately-tuned external magnetic field one can compensate for the induces level splitting and, thus, recover the Kondo effect. For this discussion, we restrict ourselves to collinear configurations.

4.1 First-Order Transport in Linear Response

Here, we only present the major steps and main results. Details of the calculations can be found in Refs. [30,31]. The first step is to relate the linear conductance $G^{\rm lin} = (\partial I/\partial V)\big|_{V=0}$ to the Green's functions of the dot. For first-order transport, we obtain

$$G^{\rm lin} = \frac{e^2}{h}\Gamma \int d\omega \, \Big\{ {\rm Im}\, G^{\rm ret}_{\downarrow\downarrow}(\omega) f'(\omega) + p \sin\frac{\phi}{2} \left[f(\omega) \frac{\partial G^{>}_{\downarrow\uparrow}(\omega)}{\partial(eV)} + [1-f(\omega)] \frac{\partial G^{<}_{\downarrow\uparrow}(\omega)}{\partial(eV)} \right] \Big\} \, . \quad (7)$$

Here, $f(\omega)$ is the Fermi function, $G_{\sigma\sigma'}(\omega)$ are the Fourier transforms of the usual retarded, greater and lesser Green's functions. Contributions involving the Green's functions $G_{\uparrow\uparrow}(\omega)$ and $G_{\uparrow\downarrow}(\omega)$ are accounted for in a prefactor 2. Since Γ already appears explicitly in front of the integral, all Green's functions are to be taken to zeroth order in Γ. In this limit, we find $-(1/\pi){\rm Im}\, G^{\rm ret}_{\downarrow\downarrow}(\omega) = (P_0^0 + P_\downarrow^\downarrow)\delta(\omega-\epsilon) + (P_\uparrow^\uparrow + P_d^d)\delta(\omega-\epsilon-U)$, $G^{>}_{\downarrow\uparrow}(\omega) = 2\pi i P_\uparrow^\downarrow \delta(\omega-\epsilon-U)$, and $G^{<}_{\downarrow\uparrow}(\omega) = 2\pi i P_\uparrow^\downarrow \delta(\omega-\epsilon)$, where $P^\chi_{\chi'} = \langle|\chi'\rangle\langle\chi|\rangle$ are elements of the stationary density matrix (to zeroth order in Γ) of the quantum-dot subsystem, with $\chi, \chi' = 0$ (empty dot), $\uparrow, \downarrow$ (singly-occupied dot), and d (doubly-occupied dot).

The main task is now to determine the density-matrix elements to zeroth order in Γ. They contain the information about the average occupation and spin on the quantum dot. The diagonal matrix elements, P^χ_χ, are nothing but the probabilities to find the quantum dot in state χ, i.e., the dot is empty with

probability $P_0 \equiv P_0^0$, singly occupied with $P_1 \equiv P_\uparrow^\uparrow + P_\downarrow^\downarrow$, and doubly occupied with $P_d \equiv P_d^d$. A finite spin can only emerge for single occupancy. The average spin $\hbar \boldsymbol{S}$ with $\boldsymbol{S} = (S_x, S_y, S_z)$ is related to the matrix elements $P_{\chi'}^{\chi}$ via $S_x = \mathrm{Re}\, P_\uparrow^\downarrow$, $S_y = \mathrm{Im}\, P_\uparrow^\downarrow$, and $S_z = (1/2)(P_\uparrow^\uparrow - P_\downarrow^\downarrow)$. To obtain the density-matrix elements by using the real-time transport theory developed in Ref. [45], we solve a kinetic equation formulated in Liouville space. The details are found in Refs. [30,31].

It is remarkable that on the r.h.s of (7), derivatives of Green's function with respect to bias voltage V appear. As a consequence, the linear conductance is not only determined by equilibrium properties of the quantum dot, but linear corrections in V are involved as well. This is consistent with the observation that, in equilibrium, the density matrix is diagonal with the matrix elements determined by the Boltzmann factors, i.e., the average spin on the quantum dot vanishes at $V = 0$ [46]. With applied bias voltage, though, a finite spin can accumulate. Therefore, to be sensitive to the relative magnetization direction of the leads, the linear conductance has to be connected to the differential spin accumulation $(d\boldsymbol{S}/dV)\big|_{V=0}$.

The results we find can be summarized as follows. At finite bias voltage, spin accumulated on the dot. Here, we only need its contribution linear in V and find

$$\left.\frac{\partial|\boldsymbol{S}|}{\partial(eV)}\right|_{V=0} = \frac{pP_1}{4k_BT}\cos\alpha(\phi)\sin\frac{\phi}{2}\,, \tag{8}$$

where P_1 is the equilibrium probability for a singly occupied dot. The spin is lying in the y-z-plane enclosing an angle α with the y-axis, where

$$\tan\alpha(\phi) = -\frac{B}{\Gamma[1 - f(\epsilon) + f(\epsilon + U)]}\cos\frac{\phi}{2}\,. \tag{9}$$

In the absence of an exchange field, the accumulated spin is oriented along $\hat{\boldsymbol{n}}_L - \hat{\boldsymbol{n}}_R$, i.e., it has a y-component only, $\alpha = 0$. The exchange field B, though, leads to a precession of the spin about the x-axis. The factor $1/\Gamma[1 - f(\epsilon) + f(\epsilon + U)]$ in (9) can be identified as the life time of the dot spin, limited by tunneling out of the dot electron or by tunneling in of a second electron with opposite spin. Since both this life time and the exchange field are of first order in Γ, the angle α acquires a finite value.

The differential spin accumulation $dS/d(eV)$ in units of k_BT is illustrated in the middle panel of Fig. 4. It is clear that single occupation of the dot is required for spin accumulation, i.e., the plotted signal is high in the valley between the two conductance peaks. The lower panel of Fig. 4 shows the evolution of the rotation angle α as a function of the level energy ϵ. This angle is large in the valley between the conductance peaks, getting close to $\pm\pi/2$. A special point is $\epsilon = -U/2$, at which, due to particle-hole symmetry, the exchange interaction vanishes. As a consequence, α shows a sharp transition from positive to negative values, accompanied with a peak in the accumulated spin.

The linear conductance is given by

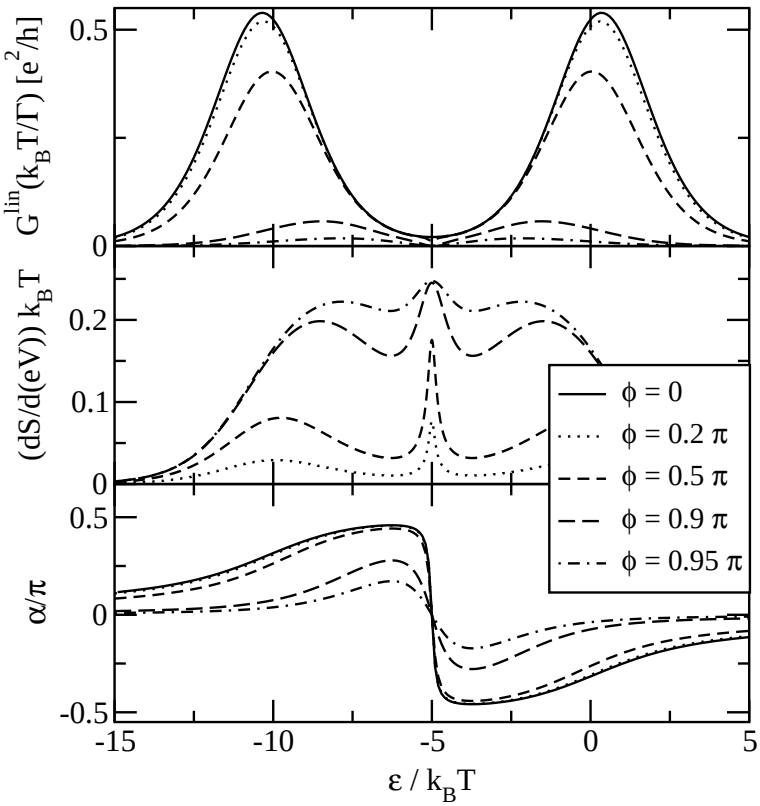

Fig. 4. Upper panel: Linear conductance (normalized by Γ/k_BT and plotted in units of e^2/h) as a function of level position ϵ for five different angles ϕ. Middle panel: Derivative of accumulated spin S with respect to bias voltage V normalized by k_BT. Lower panel: angle α between the quantum-dot spin and the y-axis. In all panels we have chosen the charging energy $U/k_BT = 10$ and $p = 1$

$$G^{\rm lin} = G^{\rm lin,max}\left(1 - p^2\cos^2\alpha(\phi)\sin^2\frac{\phi}{2}\right). \tag{10}$$

The conductance is maximal for parallel magnetization, $\phi = 0$. Its value is $G^{\rm lin,max} = (\pi e^2/h)(\Gamma/k_BT)[1-f(\epsilon+U)]f(\epsilon)[1-f(\epsilon)+f(\epsilon+U)]/[f(\epsilon)+1-f(\epsilon+U)]$. The upper panel of Fig. 4 depicts the linear conductance for five different values of the angle ϕ. For parallel magnetization, $\phi = 0$, there are two conductance peaks located near $\epsilon = 0$ and $\epsilon = -U$, respectively. With increasing angle ϕ, transport is more and more suppressed due to the spin-valve effect. However, this suppression is not uniform, as would be in the absence of the exchange field. In contrast, the spin-valve effect is less pronounced in the valley between the two peaks, where the rotation angle α is large. A large angle α reduces both the magnitude of the accumulated spin, as discussed above, and the relative angle to the magnetization of the drain electrode. Both enhance transport as compared to

the situation without the exchange field. As a consequence, the two conductance peaks move towards each other with increasing ϕ.

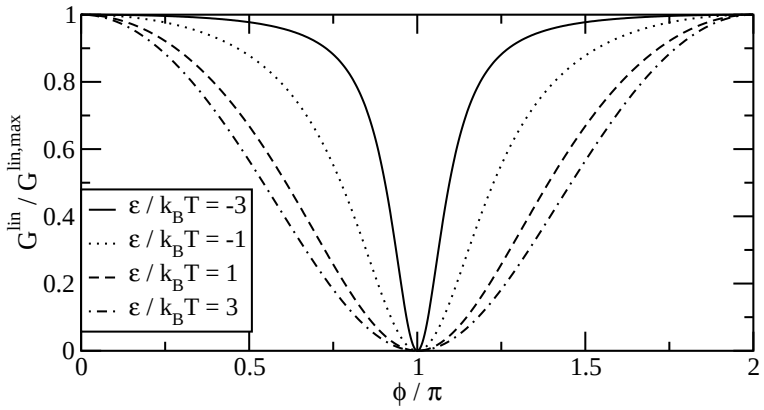

Fig. 5. Normalized linear conductance as a function of ϕ for $U/k_BT = 10$, $p = 1$, and four different values of the level position

Another way to illustrate the influence of the exchange field is to plot the ϕ-dependence of the linear conductance, see Fig. 5. For values of the level position ϵ at which the rotation angle α is small, $\epsilon/k_BT = 3$ and 1, the ϕ-dependence of the conductance is almost harmonic, as it is for single magnetic tunnel junction. For $\epsilon/k_BT = -1$ and -3, however, the spin-valve effect is strongly reduced, and conductance is enhanced, except in the regime close to antiparallel magnetization, $\phi = \pi$. The conductance, then, stays almost flat over a broad range, and then establishes the spin-valve effect only in a small region around $\phi = \pi$.

4.2 First-Order Transport in Nonlinear Response

A rather complete analysis of first-order transport through quantum-dot spin valves, which covers both the linear- and nonlinear-response regime is presented in Ref. [31]. There, we derive generalized rate equations for the dot's occupation and accumulated spin, which provide the basis of quite an intuitive understanding of the behavior of the quantum-dot state.

In the non-linear-response regime, the physics of spin accumulation is more involved as for linear response. The accumulated spin tends to align anti-parallel to the drain electrode, leading to a spin blockade, i.e., a stronger spin-valve effect. This contrasts with the exchange field which, by rotation of the accumulated spin, tends to weaken the spin-valve effect. By the interplay of these two countersteering mechanisms, a very pronounced negative differential conductance is predicted.

4.3 Second-Order Transport

While first-order transport does not probe the spin splitting generated by the exchange field, second-order transport does. Therefore, in second-order transport, the exchange splitting plays a role even for collinear configuration of the leads' magnetizations. For parallel alignment, the exchange field gives rise to a gate-voltage dependent, finite spin polarization of the dot, $n_\uparrow \neq n_\downarrow$, even at zero bias. This polarization vanishes (at zero bias) for antiparallel orientation and symmetric coupling, since, in this case, the total exchange field adds up to zero. A detailed analysis of this transport regime will be presented in Ref. [32], which includes, among other things, the prediction and explanation of a peculiar zero-bias behavior for some circumstances.

4.4 The Kondo Effect

A very sensitive probe to the exchange field is provided by the Kondo effect, which occurs in singly-occupied quantum dots below a characteristic temperature, $k_\mathrm{B}T \leq k_\mathrm{B}T_\mathrm{K} \ll \Gamma$. The singly-occupied dot defines a local spin with two degenerate states, spin up and down. The local spin can be flipped by higher-order tunneling processes, in which the electron tunnels out of the dot, and another one with opposite spin enters from one of the leads. By these processes, the dot- and the lead-electron spins are coupled to each other. At low temperature, a highly-correlated state is formed, in which the local spin is totally screened. This Kondo-correlated state is accompanied with an increased transmission through the dot, and gives rise to a sharp zero-bias anomaly in the current-voltage characteristics.

How does a finite spin polarization in the leads modify this picture? As it turns out, there are two mechanisms influencing the Kondo effect. First, the exchange field lifts the spin degeneracy on the quantum dot. This is analogous to the situation of a Kondo dot in the presence of an external magnetic field. For the latter it is well known, that the zero-bias anomaly splits by twice the Zeeman energy. Due to the same reason, the exchange-field induces a splitting of the zero-bias anomaly for our model system, but now in the absence of an external magnetic field. In the presence of an external magnetic field both exchange- and magnetic-field induced splittings contribute. In particular, for a properly-tuned magnetic field the level splitting is compensated, and a single zero-bias anomaly is recovered.

The second mechanism by which the finite spin-polarization influences the Kondo effect is the screening of the quantum-dot spin. Naturally, both up- and down-spin electrons in the leads are crucial for the screening. An imbalance of majority and minority spins in the leads, therefore, weakens the screening capability. As we will see below, this leads to a reduced Kondo temperature $T_\mathrm{K}(p)$, which even vanishes for $p = 1$.

Recently, the possibility of the Kondo effect in a quantum dot attached to ferromagnetic electrodes was discussed in a number of publications [33–39], and it was shown, that the Kondo resonance is split and suppressed in the presence of

ferromagnetic leads [37–39]. It was shown that this splitting can be compensated by an appropriately tuned external magnetic field to restore the Kondo effect [37,38], as we discuss in detail below.

In the following, we mainly concentrate on the case of parallel alignment of the leads' magnetization. For antiparallel alignment and symmetric coupling to the left and right lead, the exchange field vanishes (at zero bias voltage), and the usual Kondo resonance as for nonmagnetic electrodes forms.

Perturbative-Scaling Approach. An analytical access to the problem, which provides an intuitive picture of the involved physics, is the perturbative-scaling approach. For detail of the following calculations we refer to Ref. [37]. We make use of the poor man's scaling technique [47], performed in two stages [48]. In the first stage, when high-energy degrees of freedom are integrated out, charge fluctuations are the dominant. Afterwards, in the second stage, we map the resulting model to a Kondo Hamiltonian, and integrate out the degrees of freedom involving spin fluctuations. As we will see, each of the two stages will account for one of the two above mentioned different mechanisms by which the spin-polarized leads influence the Kondo effect, respectively.

The scaling procedure starts at an upper cutoff D_0, given by the onsite repulsion U. Charge fluctuations lead to a renormalization of the level position ϵ_σ according to the scaling equations

$$\frac{d\epsilon_\sigma}{d\ln(D_0/D)} = |t|^2 \rho_{\bar{\sigma}} \,, \tag{11}$$

where $\bar{\sigma}$ is opposite to σ. Since the renormalization is spin dependent, a spin splitting is generated. In the presence of a magnetic field, this generated spin splitting simply adds to the initial Zeeman splitting $\Delta\epsilon$. We obtain the solution $\Delta\widetilde{\epsilon} = \widetilde{\epsilon}_\uparrow - \widetilde{\epsilon}_\downarrow = -(1/\pi)p\Gamma\ln(D_0/D) + \Delta\epsilon$. The scaling of (11) is terminated [48] at $\widetilde{D} \sim -\widetilde{\epsilon}$. When plugging in $D_0 = U$ and $D = \epsilon$, we recover that the generated level splitting exactly reflects the zero-temperature limit of the exchange field (6).

To reach the strong-coupling limit, we tune the external magnetic field $B_{\rm ext}$ such that the total effective Zeeman splitting vanishes, $\Delta\widetilde{\epsilon} = 0$. In the second stage of Haldane's procedure [48], spin fluctuations are integrated out. To accomplish this, we perform a Schrieffer-Wolff transformation [11] to map the Anderson model (with renormalized parameters $\widetilde{D}$ and $\widetilde{\epsilon}$) to a Kondo Hamiltonian, see (4). Since we are interested in low-energy excitations only, we neglect the energy dependence of the coupling constants and arrive at

$$\begin{aligned} H_{\rm Kondo} = {} & J_+ S^+ \sum_{rr'kq} a^\dagger_{rk\downarrow} a_{r'q\uparrow} + J_- S^- \sum_{rr'kq} a^\dagger_{rq\uparrow} a_{r'k\downarrow} \\ & + S^z \left(J_{z\uparrow} \sum_{rr'qq'} a^\dagger_{rq\uparrow} a_{r'q'\uparrow} - J_{z\downarrow} \sum_{rr'kk'} a^\dagger_{rk\downarrow} a_{r'k'\downarrow} \right) , \end{aligned} \tag{12}$$

plus terms independent of either dot spin or lead electron operators, with $J_+ = J_- = J_{z\uparrow} = J_{z\downarrow} = |t|^2/|\widetilde{\epsilon}| \equiv J_0$ in the large-U limit. Although initially identical, the three coupling constants $J_+ = J_- \equiv J_\pm$, $J_{z\uparrow}$, and $J_{z\downarrow}$ are renormalized differently during the second stage of scaling. The scaling equations are

$$\frac{d(\rho_\pm J_\pm)}{d\ln(\widetilde{D}/D)} = \rho_\pm J_\pm(\rho_\uparrow J_{z\uparrow} + \rho_\downarrow J_{z\downarrow}) \tag{13}$$

$$\frac{d(\rho_\sigma J_{z\sigma})}{d\ln(\widetilde{D}/D)} = 2(\rho_\pm J_\pm)^2 \tag{14}$$

with $\rho_\pm = \sqrt{\rho_\uparrow \rho_\downarrow}$, $\rho_\sigma \equiv \sum_r \rho_{r\sigma}$. To solve these equations we observe that $(\rho_\pm J_\pm)^2 - (\rho_\uparrow J_{z\uparrow})(\rho_\downarrow J_{z\downarrow}) = 0$ and $\rho_\uparrow J_{z\uparrow} - \rho_\downarrow J_{z\downarrow} = J_0 p(\rho_\uparrow + \rho_\downarrow)$ is constant as well. I.e., there is only one independent scaling equation. All coupling constants reach the stable strong-coupling fixed point $J_\pm = J_{z\uparrow} = J_{z\downarrow} = \infty$ at the Kondo energy scale, $D \sim k_B T_K$. For the parallel configuration, the Kondo temperature in leading order,

$$T_{\rm K}(P) \approx \widetilde{D} \exp\left\{ -\frac{1}{(\rho_\uparrow + \rho_\downarrow) J_0} \frac{\operatorname{artanh}(p)}{p} \right\} , \tag{15}$$

depends on the polarization p in the leads. It is maximal for nonmagnetic leads, $p = 0$, and vanishes for $p \to 1$.

The unitary limit for the P configuration can be achieved by tuning the magnetic field appropriately, as discussed above. In this case, the maximum conductance through the quantum dot is $G^P_{{\rm max},\sigma} = e^2/h$ per spin, i.e., the same as for nonmagnetic leads.

Numerical Renormalization Group. Although perturbative scaling provides an instructive insight in the relevant physical mechanisms, it is a approximate method, and its reliability is, a priori, not clear. The numerical renormalization-group (NRG) technique [11], on the other hand, is one of the most accurate methods available to study strongly-correlated systems in the Kondo regime. Recently, it was adapted to the case of a quantum dot coupled to ferromagnetic leads [38,39].

The NRG study [38,39] confirms the predictions of the perturbative scaling analysis. The Kondo resonance is split, as a consequence of the exchange field. By appropriately tuning an external magnetic field, this splitting can be fully compensated and the Kondo effect can be restored [38]. Precisely at this field, the occupancy of the local level is the same for spin up and down, $\langle n_\uparrow \rangle = \langle n_\downarrow \rangle$, a fact that follows from the Friedel sum rule. Moreover, the Kondo effect has unusual properties such as a strong spin polarization of the Kondo resonance and for the density of states. Nevertheless, the quantum dot conductance is found to be the same for each spin channel, $G_\uparrow = G_\downarrow$. Furthermore, by analyzing the spin spectral function, the Kondo temperature can be determined, and the functional dependence on p as given by (15) has been confirmed.

More recently, the NRG scheme has been extended to account for structured densities of states [40]. The generated spin splitting found in this case is found to coincide with the exchange field defined in (6), when the energy-dependent density of states is included in the integral.

Nonequilibrium Transport Properties. To get a qualitative understanding of how the exchange field appears in nonlinear transport, we employ an equations-of-motions scheme with the usual decoupling scheme [49], but generalized by a self-consistent determination of the level energy to account for the exchange field in a correct way. We skip all technical details here (they are given in Ref. [37]), and go directly to the discussion of the results.

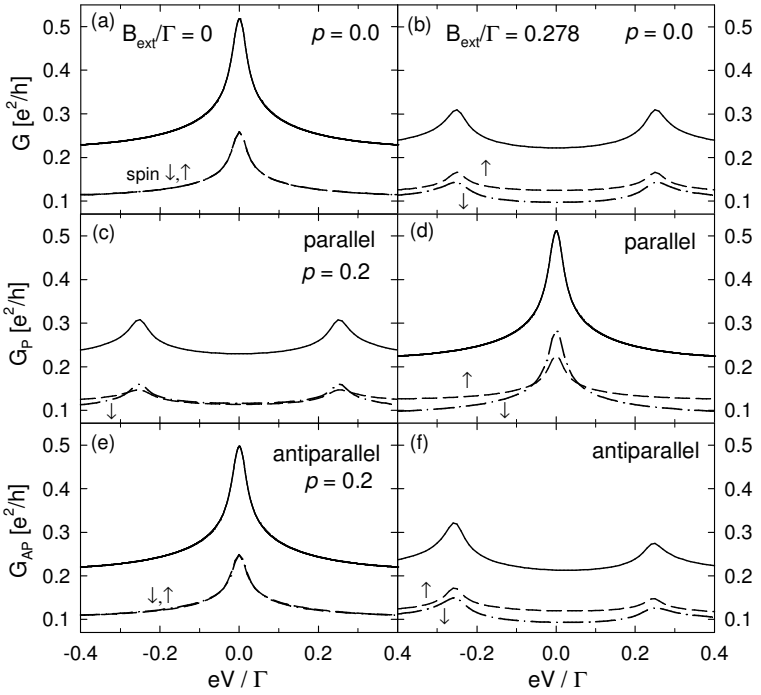

Fig. 6. Total differential conductance (solid lines) as well as the contributions from the spin up (dashed) and the spin down (dotted-dashed) channel vs. applied bias voltage V at zero magnetic field $B_{\rm ext} = 0$ (a,c,e) and at finite magnetic field (b,d,f) for normal (a,b) and ferromagnetic leads with parallel (c,d) and antiparallel (e,f) alignment of the lead magnetizations. The degree of spin polarization of the leads is $p = 0.2$ and the other parameters are: $k_{\rm B}T/\Gamma = 0.005$ and $\epsilon/\Gamma = -2$

In Fig. 6 we show the differential conductance as a function of the transport voltage. For nonmagnetic leads, there is a pronounced zero-bias maximum [Fig. 6(a)], which splits in the presence of a magnetic field [Fig. 6(b)]. For magnetic leads and parallel alignment, we find a splitting of the peak in the absence

of a magnetic field [Fig. 6(c)], which can be tuned away by an appropriate external magnetic field [Fig. 6(d)]. In the antiparallel configuration, the opposite happens, no splitting at $B_{\rm ext} = 0$ [Fig. 6(e)] but finite splitting at $B_{\rm ext} > 0$ [Fig. 6(f)] with an additional asymmetry in the peak amplitudes as a function of the bias voltage.

We conclude by mentioning that very recent experimental results [24,25] indicate confirmation of our theoretical predictions.

5 Summary

The interplay of charge and spin degrees of freedom in quantum dots coupled to ferromagnetic leads is investigated theoretically. The simultaneous presence of both spin polarization in the leads and strong Coulomb interaction in the quantum dot generates an exchange field that acts on the quantum-dot electrons. We analyze its influence on the dot state and the conductance for different transport regimes. Two mechanisms, which can be important, are identified. The exchange field can precess an accumulated quantum-dot spin, and it generates a level splitting. In the limit of weak dot-lead coupling, the spin precession leads to a nontrivial dependence of the linear conductance on the angle between the leads' magnetization. For strong dot-lead coupling, the exchange field is detectable in a splitting of the Kondo resonance, which can be tuned away by additionally applying an external magnetic field.

6 Acknowledgments

The presented work is based on joint publications with L. Borda, M. Braun, R. Bulla, J. von Delft, H. Imamura, S. Maekawa, M. Sindel, Y. Utsumi, and I. Weymann, all of whom we thank for fruitful collaboration.

We thank G. Bauer, A. Brataas, P. Bruno, T. Costi, A. Fert, L. Glazman, W. Hofstetter, B. Jones, C. Marcus, J. Nygård, A. Pasupathy, D. Ralph, A. Rosch, S. Takahashi, D. Urban, and M. Vojta for discussions. This work was supported by the Deutsche Forschungsgemeinschaft under the Center for Functional Nanostructures and the Emmy-Noether program, and by the European Community under the 'Spintronics' RT Network of the EC RTN2-2001-00440, Project PBZ/KBN/044/P03/2001, and the Centre of Excellence for Magnetic and Molecular Materials for Future Electronics within the EC Contract G5MA-CT-2002-04049.

References

1. S.A. Wolf, D.D. Awschalom, R.A. Buhrman, J.M. Daughton, S. von Molnar, M.L. Roukes, A.Y. Chtchelkanova, D.M. Treger: Science **294**, 1488 (2001)
2. *Semiconductor Spintronics and Quantum Computation*, ed. by D.D. Awschalom, D. Loss, and N. Samarth (Springer, Berlin 2002)

3. S. Maekawa, T. Shinjo: *Spin Dependent Transport in Magnetic Nanostructures* (Taylor & Francis 2002)
4. D.V. Averin, K.K. Likharev: in *Mesoscopic Phenomenon in Solids*, ed. by B.L. Altshuler, P.A. Lee, R.A. Webb (Amsterdam: North-Holland 1991)
5. *Single Charge Tunneling: Coulomb Blockade Phenomena in Nanostructures*, NATO ASI Series B: Physics 294, ed. by H. Grabert, M.H. Devoret (Plenum Press, New York 1992)
6. *Mesoscopic Electron Transport*, ed. by L.L. Sohn, L.P. Kouwenhoven, G. Schön (Kluwer, Dordrecht 1997)
7. M. Jullière: Phys. Lett. A **54**, 225 (1975)
8. J.C. Slonczewski: Phys. Rev. B **39**, 6995 (1989)
9. J.S. Moodera, L.R. Kinder: J. Appl. Phys. **79**, 4724 (1996); H. Jaffrès, D. Lacour, F. Nguyen Van Dau, J. Briatico, F. Petroff, A. Vaurès: Phys. Rev. B **64**, 064427 (2001)
10. S. Datta, B. Das: Appl. Phys. Lett. **56**, 665 (1990)
11. A.C. Hewson: *The Kondo Problem to Heavy Fermions* (Cambridge Univ. Press 1993)
12. L.F. Schelp, A. Fert, F. Fettar, P. Holody, S.F. Lee, J.L. Maurice, F. Petroff, A. Vaurs: Phys. Rev. B **56**, 5747 (1997)
13. H. Brückl, G. Reiss, H. Vinzelberg, M. Bertram, I. Mönch, J. Schumann: Phys. Rev. B **58**, 8893 (1998)
14. K. Ono, H. Shimada, S. Kobayashi, Y. Ootuka: J. Phys. Soc. Jpn. **65**, 3449 (1996); K. Ono, H. Shimada, Y. Ootuka, J. Phys. Soc. Jpn. **66**, 1261 (1997)
15. S. Mitani, S. Takahashi, K. Takanashi, K. Yakushiji, S. Maekawa, H. Fujimori: Phys. Rev. Lett. **81**, 2799 (1998); H. Imamura, J. Chiba, S. Mitani, K. Takanashi, S. Takahashi, S. Maekawa, H. Fujimori: Phys. Rev. B **61**, 46 (2000); K. Yakushiji, S. Mitani, K. Takanashi, S. Takahashi, S. Maekawa, H. Imamura, H. Fujimori: Appl. Phys. Lett. **78**, 515 (2001)
16. K. Yakushiji, S. Mitani, K. Takanashi, H. Fujimori: J. Appl. Phys. **91**, 7038 (2002)
17. C.D. Chen, Y.D. Yao, S.F. Lee, J.H. Shyu: J. Appl. Phys. **91**, 7469 (2002)
18. Y. Chye, M.E. White, E. Johnston-Halperin, B.D. Gerardot, D.D. Awschalom, P.M. Petroff: Phys. Rev. B **66**, 201301(R) (2002)
19. M.M. Deshmukh, D.C. Ralph: Phys. Rev. Lett. **89**, 266803 (2002)
20. R. Jansen, J.S. Moodera: Appl. Phys. Lett. **75**, 400 (1999); S. Tanoue, A. Yamasaki: J. Appl. Phys. **88**, 4764 (2000)
21. J. Nygård, D.H. Cobden, P.E. Lindelof: Nature **408**, 342 (2000)
22. M.R. Buitelaar, T. Nussbaumer, C. Schönenberger: Phys. Rev. Lett. **89**, 256801 (2002)
23. A. Jensen, J. Nygård, J. Borggreen: in *Proceedings of the International Symposium on Mesoscopic Superconductivity and Spintronics*, ed. by H. Takayanagi, J. Nitta (World Scientific 2003) pp. 33-37; B. Zhao, I. Mönch, H. Vinzelberg, T. Mühl, C.M. Schneider: Appl. Phys. Lett. **80**, 3144 (2002); J. Appl. Phys. **91**, 7026 (2002); K. Tsukagoshi, B.W. Alphenaar, H. Ago: Nature **401**, 572 (1999)
24. J. Nygård, C.C. Markus, private communication.
25. D.C. Ralph, A. Pasupathy, private communnication.
26. Y. Manassen, R.J. Hamers, J.E. Demuth, A.J. Castellano: Phys. Rev. Lett. **62**, 2531 (1989); C. Durkan, M.E. Welland: Appl. Phys. Lett. **80**, 458 (2002)
27. J. Barnaś, A. Fert: Phys. Rev. Lett. **80**, 1058 (1998); S. Takahashi, S. Maekawa: Phys. Rev. Lett. **80**, 1758 (1998); A. Brataas, Yu.V. Nazarov, J. Inoue, G.E.W. Bauer: Phys. Rev. B **59**, 93 (1999); M. Pirmann, J. von Delft, G. Schön:

J. Mag. Mag. Mat. **219**, 104 (2000); J. Barnaś, J. Martinek, G. Michalek, B.R. Bulka, A. Fert: Phys. Rev. B **62**, 12363 (2000); J. Martinek, J. Barnaś, S. Maekawa, H. Schoeller, G. Schön: Phys. Rev. B **66**, 014402 (2002)
28. W. Rudziński, J. Barnaś: Phys. Rev. B **64**, 085318 (2001); G. Usaj, H.U. Baranger: Phys. Rev. B **63**, 184418 (2001); A. Cottet, W. Belzig, C. Bruder: cond-mat/0308564
29. J. Martinek, J. Barnaś, A. Fert, S. Maekawa, G. Schön: J. Appl. Phys. **93**, 8265 (2003)
30. J. König, J. Martinek: Phys. Rev. Lett. **90**, 166602 (2003)
31. M. Braun, J. König, J. Martinek: submitted to Phys. Rev. B.
32. I. Weymann, J. Martinek, J. König, J. Barnaś, G. Schön: to be published.
33. N. Sergueev, Q.F. Sun, H. Guo, B.G. Wang, J. Wang: Phys. Rev. B **65**, 165303 (2002)
34. P. Zhang, Q.K. Xue, Y. Wang, X.C. Xie: Phys. Rev. Lett. **89**, 286803 (2002)
35. B.R. Bułka, S. Lipinski: Phys. Rev. B **67**, 024404 (2003)
36. R. Lopez, D. Sanchez: Phys. Rev. Lett. **90**, 116602 (2003)
37. J. Martinek, Y. Utsumi, H. Imamura, J. Barnaś, S. Maekawa, J. König, G. Schön: Phys. Rev. Lett. **91**, 127203 (2003)
38. J. Martinek, M. Sindel, L. Borda, J. Barnaś, J. König, G. Schön, J. von Delft: Phys. Rev. Lett. **91**, 247202 (2003)
39. M.S. Choi, D. Sanchez, R. Lopez: Phys. Rev. Lett. **92**, 056601 (2004)
40. J. Martinek, M. Sindel, L. Borda, J. Barnaś, R. Bulla, J. König, G. Schön, S. Maekawa, J. von Delft, to be published
41. K. Yosida: *Theory of Magnetism* (Springer, Berlin 1996).
42. *Handbook of the Band Structure of Elemental Solids*, ed. by D.A. Papaconstantopoulos (Plenum Press 1986)
43. J. König, Y. Gefen: Phys. Rev. Lett. **86**, 3855 (2001); Phys. Rev. B **65**, 045316 (2002); B. Kubala, J. König, Phys. Rev. B **65**, 245301 (2002)
44. We note that, for all the effects discussed in this paper, the (spin-dependent) density of states ρ_σ and the (spin-independent) tunneling amplitudes t enter via the combination $\rho_\sigma |t|^2$. As a consequence, all the conclusions drawn in this paper are valid also for a system with spin-dependent tunneling amplitudes but nonmagnetic leads, or a mixture of both.
45. J. König, H. Schoeller, G. Schön: Phys. Rev. Lett. **76**, 1715 (1996); J. König, J. Schmid, H. Schoeller, G. Schön: Phys. Rev. B **54**, 16820 (1996); H. Schoeller, in Ref. [6]; J. König: *Quantum Fluctuations in the Single-Electron Transistor* (Shaker, Aachen 1999)
46. In equilibrium and zeroth order in Γ, the average spin on the dot vanishes: majority-spin electrons enter the quantum dot at a higher rate than minority spins, but this is exactly compensated by a higher rate for the majority spins to leave the dot.
47. P.W. Anderson: J. Phys. C **3**, 2439 (1970)
48. F.D.M. Haldane: Phys. Rev. Lett. **40**, 416 (1978)
49. Y. Meir, N.S. Wingreen, P.A. Lee: Phys. Rev. Lett. **70**, 2601 (1993); N.S. Wingreen, Y. Meir: Phys. Rev. B **49**, 11040 (1994)